Chemical and Process Engineering: New Frontiers, 2025, 46(2), e95
DOI: 10.24425/cpe.2025.153680

# Iron-based pigments on zeolite and clay minerals

Barbara Michorczyk*, Dominika Baran

Cracow University of Technology, Faculty of Chemical Engineering and Technology, Warszawska 24, 31-155 Kraków, Poland

* **Corresponding author, e-mail:** barbara.michorczyk@pk.edu.pl

**Article info:**
Received: 01 May 2025
Revised: 03 June 2025
Accepted: 05 June 2025

**Abstract**
A series of inexpensive, stable, and environmentally friendly iron pigments was synthesized based on zeolite and clay minerals. For the synthesis of pigments, zeolite – clinoptilolite and clay minerals: bentonite and kaolin were used and as a source of iron ions – iron chloride. The influence of the type of clay minerals/zeolite used and the preparation method on the color of the obtained pigments and the resistance of the produced material to factors such as: UV radiation, organic solvents, alkalis and acids were studied. The use of different synthesis methods and various clay minerals or zeolite for the preparation of iron-based pigments enabled the formation of a wide range of colors, varying from beige and red to different shades of brown. The non-toxicity and good stability of the obtained pigments combined with the low cost of their production make them have great potential for use in many areas, such as ceramics, painting and others.

**Keywords**
hybrid pigment; kaolin; bentonite; clinoptilolite; iron oxide

## 1. INTRODUCTION

Iron-based pigments have been utilized since prehistoric times. They are obtained from both natural mineral sources and, to meet growing demand, are also produced through chemical synthesis. Among synthetic iron oxide pigments, hematite ($\alpha$-$Fe_2O_3$) is one of the most widely applied, cost-effective, and non-toxic red pigments (Tian et al., 2017b). The main advantage of iron pigments is their high resistance to light and diverse environmental conditions, as well as their good hiding power. In addition, they exhibit favorable dispersibility across multiple formulation systems. These properties contribute to their broad application across various industrial sectors, including the production of ceramics, inks, paints, coatings, toners, construction materials, and plastics, as well as in cosmetics and pharmaceuticals (Pfaff, 2022; Tian et al., 2017a; Tian et al., 2017b; Tora et al., 2009). Recent studies have indicated that a promising research direction is the synthesis of pigments using natural mineral raw materials, which could make pigment production more cost-effective (Roy et al., 2015) and additionally enable the expansion of the color palette and the modification of their physicochemical properties.

Among clay minerals, kaolin is widely used in paint production due to its chemical inertness, high covering power, ability to impart desirable flow properties, as well as its low cost and non-toxicity (Buyondo et al., 2022). The incorporation of metal oxides such as Cu(II), Ni(II), Cr(III), and Fe(III) into kaolin-based composites can result in promising ceramic pigment materials suitable for use in paints (Roy et al. 2022).

Another important clay mineral is bentonite. It is a type of clay composed primarily of smectite, particularly montmorillonite – a layered silicate mineral. This structure is responsible for properties such as high cation exchange capacity, large surface area, and swelling capacity. Bentonite may also contain other clay minerals, such as illite, as well as non-clay minerals including quartz and feldspar (Cunha et al., 2023; Mota-Heredia et al., 2024). Various changes in the physical and chemical properties of bentonite were observed upon contact with ferric chloride. These included an increase in water content, a reduction in specific surface area and a decrease in cation exchange capacity. In addition, secondary minerals such as akaganeite, goethite, and hematite were formed. In the case of smectites, structural modifications were observed, including an enrichment in iron content (Mota-Heredia et al., 2024). In addition, it was found that the addition of $SiO_2$ intensified the red coloration of the pigments (Tian et al., 2017a), and the silicate sources can be clay minerals and zeolites. Hosseini-Zori et al. (2008) demonstrated, based on colorimetric analysis using the CIE-L*a*b* system that the red ceramic pigment ($SiO_2$–$Fe_2O_3$), synthesized by incorporating hematite into a fumed silica matrix, exhibited high Hunter $a^*$ values (10.0–37.0), which are indicative of a strong red hue. Tian et al. (2017a; 2017b) synthesized a series of hybrid red pigments based on sepiolite, halloysite, and attapulgite. These pigments exhibited high $a^*$ values of 25.1, 34.4, and 36.3, respectively, indicating strong red color performance, which was superior to that of comparable commercial red pigments (Tian et al. 2017b). Zeolites are also of interest for pigment production. Under high-temperature conditions, the zeolite structure disintegrates, resulting in a transformation into either amorphous or crystalline ceramic materials, depending on their chemical composition. The incorporation of transition metal cations into the zeolite structure is particularly noteworthy, as it can impart characteristic colors that are retained even after heat treatment (Fatah et al., 2024). In addition, the homogeneous distribution of cations within the zeolite structure ensures more consistent, uniform, and stable coloration of the product (Fatah et al., 2024). Fatah

et al. (2024) obtained brown, blue and green pigments by modifying zeolites (mainly clinoptilolite) with Zn and Co ions, followed by calcination at various temperatures. In turn, Dejoie et al. (2010) developed an indigo@silicalite hybrid pigment based on an MFI-type zeolite, characterized by high color durability. The use of zeolites and clay minerals in pigment production enables the development of materials with bright colors and high color stability, while also allowing for color modification, extension of the color palette, enhancement of desired physicochemical properties and often a reduction in production costs. Moreover, the desirable physical and physicochemical properties of clay minerals have enabled their substantial application in pharmaceutical and cosmetic formulations (Khurana et al., 2015). Natural zeolites – particularly clinoptilolite – have also been widely utilized in these fields (Pesando et al., 2022). Therefore, in this study focused on the synthesis of a series of iron-based pigments using clay minerals (bentonite and kaolin) and the zeolite clinoptilolite. The pigments were prepared using two methods: chemical precipitation and a one-step hydrothermal process without the addition of a chemical precipitant. All reagents used to synthesize the described pigments are non-toxic, and additionally, the clay minerals used can act as environmentally friendly precipitants during the hydrothermal reaction serving also as "micro-reactors" for forming $Fe_2O_3$ crystals and inhibiting the aggregation of $Fe_2O_3$ particles (Lu et al., 2018). The effects of the preparation method, calcination temperature, and iron ion concentration on the color, its durability, and phase composition of the resulting pigments were investigated.

## 2. EXPERIMENTAL

### 2.1. Materials

The reagents were obtained from the following sources: bentonite – Acros Organics B.V.B.A.; clinoptilolite – Nanga; kaolin and $FeCl_2 \cdot 6H_2O$ – Sigma-Aldrich; NaOH, HCl, and C6H5CH3 – POCH S.A.; 96% C2H5OH – Chempur. Distilled water was used for the preparation of all materials.

### 2.2. Synthesis of pigments

The pigments were synthesized using two approaches: (i) a precipitation method employing NaOH as the precipitating agent, and (ii) a one-step process without the use of a precipitating agent, following a modified procedure based on Tian et al. (2017a; 2017b). A series of iron-based pigments with clay mineral/zeolite to iron(II) chloride weight ratios of 4:5 were prepared as follows: an aqueous solution of iron(II) chloride was added to a suspension containing a clay mineral (bentonite or kaolin) or zeolite (clinoptilolite), and the mixture was stirred using a magnetic stirrer at room temperature for 30 minutes. The pH was adjusted to 7 by adding a 10% NaOH solution. The resulting suspension was then subjected to ultrasonic treatment at 80 °C for 30 minutes. After cooling, the mixture was filtered and washed with deionized water. The obtained solids were dried for 10 hours at 100 °C and subsequently calcined at 500 °C for 8 hours, with a heating rate of 1.5 °C/min. Additionally, pigments with a weight ratio of 4:5 were synthesized using a one-step hydrothermal method without the addition of a precipitating agent. The synthesis was conducted in a stainless steel reactor equipped with a Teflon liner. A mixture containing an aqueous solution of iron(II) chloride and the respective clay mineral or zeolite was stirred using a magnetic stirrer for 30 minutes, followed by ultrasonic treatment at 80 °C for 30 minutes. The resulting suspension was then transferred to the reactor and heated at 180 °C for 21 hours, with a heating rate of 1 °C/min. The final product was filtered and dried at 100 °C for 10 hours. The dried pigments were ground and sieved to obtain a particle size fraction of 0.2 mm. The following designations were used for the individual materials in this study: Fe–Clinoptilolite–P, Fe–Bentonite–P, Fe–Kaolin–P, Fe–Clinoptilolite–PK, Fe–Bentonite–PK, Fe–Kaolin–PK, Fe–Clinoptilolite–HT, Fe–Bentonite–HT, and Fe–Kaolin–HT, where 'P' denotes a pigment obtained by the precipitation method, 'PK' indicates samples calcined at 500 °C, and 'HT' refers to materials synthesized via the hydrothermal method.

### 2.3. Stability tests

To evaluate the chemical stability of the obtained materials, the samples were exposed to 0.1 M HCl, 0.1 M NaOH, ethanol, and toluene. Typically, 0.5 g of each pigment was immersed in 50 mL of one of the selected reagents and left for 48 hours. After exposure, the samples were filtered and dried. To assess the resistance of the pigments to UV radiation, they were irradiated using a 39 W LED lamp for 10 hours. The color of the fresh and treated hybrid pigments was evaluated using colorimetric analysis based on the CIE-L*a*b* color space. The $L^*$ value indicates the lightness of the sample, while the $a^*$ (red–green axis) and $b^*$ (yellow–blue axis) values qualitatively describe its chromaticity (Tian et al., 2017b). Color measurements were carried out using a CR8 3nh spectrocolorimeter. The color difference ($\Delta E$) between two samples in the CIE-L*a*b* color space is calculated using the following equation:

$$\Delta E = \sqrt{(\Delta L)^2 + (\Delta a)^2 + (\Delta b)^2} \quad (1)$$

### 2.4. Characterizations

The phase composition of the pigments was determined using X-ray diffraction. XRD patterns were collected from 5 to 80°. XRD studies were performed at ambient temperature using a SmartLab SE equipped with a semiconductor (2D) X-ray detector HyPix 400 and a Cu LFF anode tube. UV-Vis spectrophotometric measurements were carried out using the diffuse reflectance spectroscopy (DRS) method with a Thermo

Scientific Evolution 220 spectrophotometer. Measurements were performed in the wavelength range of 250–900 nm, with the following instrument settings: integration time – 0.3 s, slit width – 2 nm, scan speed – 400 nm/min, and data interval – 2 nm. The CIE-L*a*b* colorimetric method was used to describe the color of the prepared pigments. The measurements were carried out using a CR8 spectrocolorimeter.

## 3. RESULTS AND DISCUSSION

### 3.1. XRD analysis

Figure 1 presents the diffractograms of kaolin and the pigments synthesized from it. In all samples, except for the Fe–Kaolin–PK sample calcined at 500 °C, the dominant phase is kaolinite.

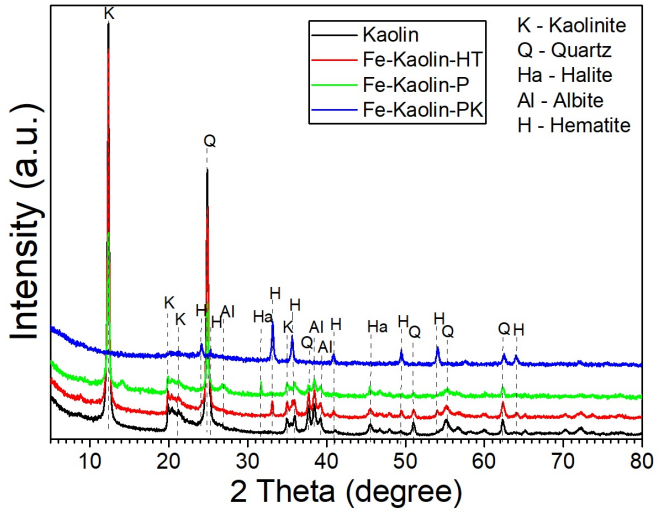


Figure 1. XRD patterns of kaolin and its derived pigments: kaolin (black line), Fe–Kaolin–HT (red line), Fe–Kaolin–P (green line), and Fe–Kaolin–PK (blue line).

In the sample calcined at 500 °C, reflections corresponding to kaolinite disappear, and hematite becomes the dominant phase. The formation and transformation of Fe oxide–kaolinite associations are significantly influenced by factors such as pH, temperature, and reaction time (Wei et al., 2011). Wei et al. (2011) demonstrated the inhibitory effect of kaolinite on the formation of crystalline Fe oxides. In the presence of kaolinite, the formation of crystalline Fe oxides required a higher temperature compared to a system without kaolinite.

X-ray diffraction (XRD) patterns of the raw bentonite and the synthesized pigments are presented in Figure 2. The XRD analysis of the bentonite revealed reflections corresponding to the crystallographic phases of montmorillonite and quartz, with montmorillonite being the dominant phase (Fig. 2) (Niziurska et al., 2022; Orolínová et al., 2009). The XRD patterns of the bentonite clay and the pigments synthesized from it differed significantly from those of the raw material. In the material obtained via the hydrothermal method, additional reflections corresponding to the crystallographic phases of rokühnite and andalusite were identified. In the pigments prepared by the precipitation method (Bentonite–P and Bentonite–PK), the reflections originating from montmorillonite either disappeared or their intensity was significantly reduced. Clear reflections corresponding to hematite were observed in the diffraction pattern of the pigment calcined at 500 °C (Bentonite–PK).

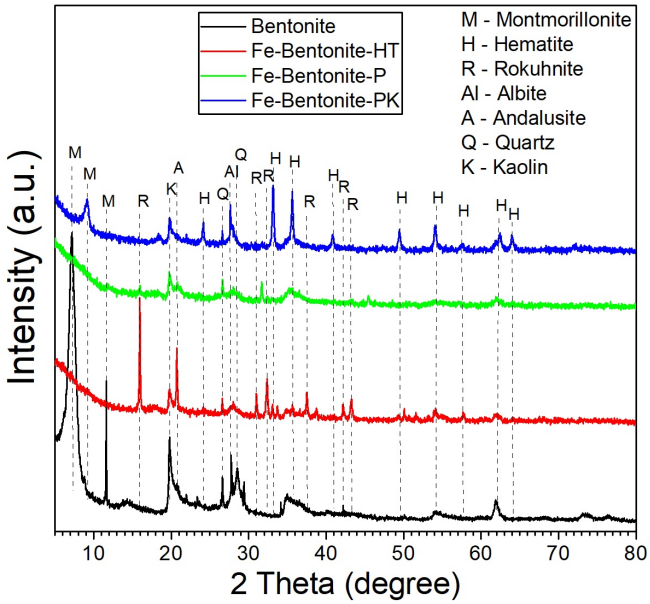


Figure 2. XRD patterns of bentonite and its derived pigments: Bentonite (black line), Fe–Bentonite–HT (red line), Fe–Bentonite–P (green line), and Fe–Bentonite–PK (blue line).

In all pigment samples synthesized on clinoptilolite, reflections attributed to the clinoptilolite structure were identified (Fig. 3). The X-ray diffractograms reveal no notable changes in the primary zeolite diffraction peaks, indicating no detectable damage to the clinoptilolite framework and the presence of a small amount of additional Fe oxide crystalline phases. The clinoptilolite structure remains stable up to approximately 700 °C, with no significant structural changes observed (Doula, 2006; Grifasi et al., 2024). In the case of bentonite and kaolinite, calcination at 500 °C leads to the disappearance of the crystallographic structures characteristic of these clay minerals and the appearance of intense reflections corresponding to hematite. In contrast, for clinoptilolite, the crystallographic structure remains almost intact.

### 3.2. UV-Vis DR spectra analysis

Figures 4–6 present the UV–Vis diffuse reflectance spectra of zeolite and clay minerals, as well as the pigments synthesized from them.

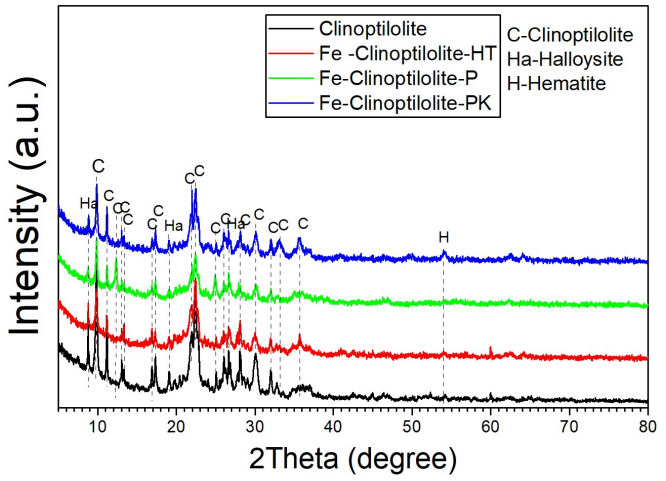


Figure 3. XRD patterns of clinoptilolite and its derived pigments: Clinoptilolite (black line), Fe–Clinoptilolite–HT (red line), Fe–Clinoptilolite–P (green line), and Fe–Clinoptilolite–PK (blue line).

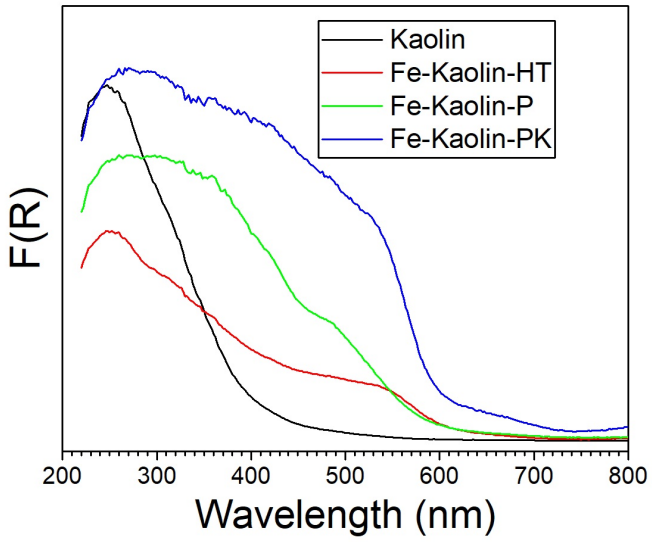


Figure 4. UV-Vis DR spectra of kaolin and its derived pigments: Kaolin (black line), Fe–Kaolin–HT (red line), Fe–Kaolin–P (green line), and Fe–Kaolin–PK (blue line).

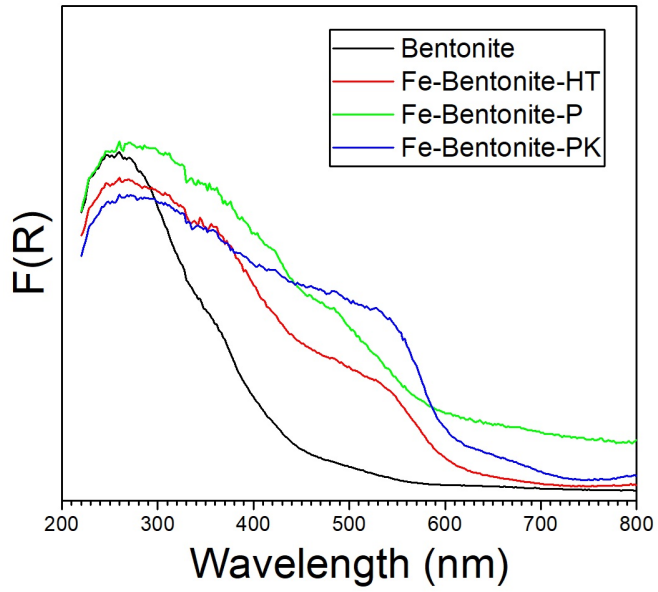


Figure 5. UV-Vis DR spectra of bentonite and its derived pigments: Bentonite (black line), Fe–Bentonite–HT (red line), Fe–Bentonite–P (green line), and Fe–Bentonite–PK (blue line).

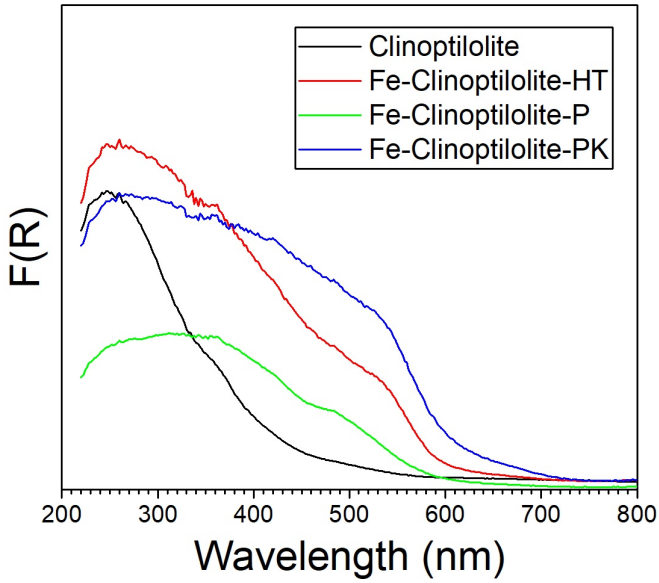


Figure 6. UV-Vis DR spectra of clinoptiolite and its derived pigments: Clinoptilolite (black line), Fe–Clinoptilolite–HT (red line), Fe–Clinoptilolite–P (green line), and Fe– Clinoptilolite–PK (blue line).

Kaolin (Fig. 4), bentonite (Fig. 5) and clinoptilolite (Fig. 6) exhibit a single narrow absorption band in the UV region, with a maximum at approximately 255 nm. In contrast, all iron-based pigments synthesized from these materials, regardless of the preparation method, display broad absorption bands characteristic of brown-coloured compounds. In the UV–Vis diffuse reflectance spectra of iron-containing samples, three characteristic absorption regions can be distinguished: the band below 300 nm is attributed to tetrahedrally (200–250 nm) and octahedrally (250–300 nm) coordinated mononuclear $Fe^{3+}$ ions; the absorption in the 300–400 nm range is associated with oligonuclear $Fe_x^{3+}O_y$ clusters; and the broad band above 400 nm corresponds to bulky $Fe_2O_3$ agglomerates (Rutkowska et al., 2014). The nature and distribution of iron species vary among the individual materials and depend not only on whether zeolite or clay minerals were used for their synthesis, but also on the preparation method – particularly the temperature – which significantly affects the distribution of iron species. In general, materials calcined at 500 °C exhibit significantly higher intensity in the band above 400 nm compared to those dried at 100 °C or synthesized hydrothermally at 180 °C. This broad band above 400 nm corresponds to the presence of bulky $Fe_2O_3$ agglomerates.

## 3.3. Color values and stability

The color characteristics of the pigments were recorded in the CIE-L*a*b* color space and are presented in Tables 1–3.

Table 1 presents data on kaolin-based pigments produced using different methods, as well as the perceptual color differences ($\Delta E$) between the fresh pigments and those exposed to various chemicals and UV radiation. The pigment calcined at 500 °C exhibits the most positive $a^*$ value (24.21), indicating

Table 1. Colorimetric coordinates of Fe–Kaolin hybrid pigments

| Pigment | Solvents (solutions)/ UV radiation | $L^*$ | $a^*$ | $b^*$ | $\Delta E$ | Color |
|---|---|---|---|---|---|---|
| Kaolin | – | 76.08 | 0.43 | 4.62 | – | |
| Fe–Kaolin–P | Before erosion | 51.66 (+/–0.56) | 13.17 (+/–0.08) | 27.92 (+/–0.37) | – | |
| | Hydrochloric acid | 53.87 (+/–0.71) | 12.35 (+/–0.13) | 25.46 (+/–0.57) | 3.41 | |
| | Sodium hydroxide | 50.35 (+/–0.39) | 13.51 (+/–0.50) | 24.74 (+/–2.19) | 3.45 | |
| | Alcohol | 51.97 (+/–0.52) | 12.80 (+/–0.57) | 25.83 (+/–1.95) | 3.45 | |
| | Toluene | 52.20 (+/–0.46) | 12.75 (+/–0.23) | 26.77 (+/–1.17) | 1.33 | |
| | 10h UV radiation | 52.91 (+/–0.35) | 12.90 (+/–0.25) | 27.29 (+/–0.65) | 1.42 | |
| Fe–Kaolin–HT | Before erosion | 53.72 (+/–0.23) | 11.99 (+/–0.05) | 8.55 (+/–0.42) | – | |
| | Hydrochloric acid | 53.75 (+/–0.13) | 12.11 (+/–0.04) | 6.58 (+/–0.02) | 1.97 | |
| | Sodium hydroxide | 51.34 (+/–0.11) | 13.23 (+/–0.06) | 8.39 (+/–0.14) | 2.68 | |
| | Alcohol | 53.26 (+/–0.17) | 12.51 (+/–0.10) | 8.08 (+/–0.06) | 0.83 | |
| | Toluene | 54.52 (+/–0.03) | 12.22 (+/–0.03) | 8.47 (+/–0.08) | 0.83 | |
| | 10h UV radiation | 54.24 (+/–0.25) | 11.63 (+/–0.58) | 7.99 (+/–0.33) | 0.84 | |
| Fe–Kaolin– PK | Before erosion | 41.62 (+/–0.88) | 24.21 (+/–0.50) | 29.73 (+/–0.54) | – | |
| | Hydrochloric acid | 44.20 (+/–0.29) | 25.57 (+/–0.10) | 31.78 (+/–0.12) | 3.56 | |
| | Sodium hydroxide | 41.32 (+/–0.81) | 23.71 (+/–0.69) | 27.43 (+/–2.10) | 2.37 | |
| | Alcohol | 38.94 (+/–0.13) | 24.27 (+/–0.19) | 29.31 (+/–0.44) | 2.71 | |
| | Toluene | 44.19 (+/–1.13) | 24.19 (+/–0.98) | 29.28 (+/–1.77) | 2.61 | |
| | 10h UV radiation | 35.06 (+/–0.56) | 23.28 (+/–0.61) | 28.95 (+/–0.87) | 6.67 | |

a stronger red color tone. As a result of calcination, the crystallographic structure of kaolin was completely transformed, with the XRD pattern dominated by reflections corresponding primarily to hematite. An interesting brown shade was obtained using the hydrothermal method. In this case, the crystallographic structure of kaolin (Fig. 1) underwent only slight changes, and additional reflections corresponding to hematite were observed. The pigment synthesized by the hydrothermal method exhibited the highest resistance to various chemicals and UV radiation, with $\Delta E$ values ranging from

Table 2. Colorimetric coordinates of Fe–Bentonite hybrid pigments

| Pigment | Solvents (solutions)/ UV radiation | $L*$ | a* | $b*$ | $\Delta E$ | Color |
|---|---|---|---|---|---|---|
| Bentonite | – | 66.11 | 1.20 | 11.60 | – | |
| Fe–Bentonite–P | Before erosion | 33.93 (+/–0.45) | 8.05 (+/–0.82) | 18.34 (+/–1.09) | – | |
| | Hydrochloric acid | 27.89 (+/–0.86) | 13.38 (+/–0.52) | 17.93 (+/–0.82) | 8.06 | |
| | Sodium hydroxide | 34.23 (+/–2.20) | 10.36 (+/–0.99) | 12.61 (+/–2.05) | 6.18 | |
| | Alcohol | 41.42 (+/–0.59) | 15.05 (+/–0.72) | 25.47 (+/–2.70) | 12.49 | |
| | Toluene | 38.49 (+/–0.48) | 13.93 (+/–0.30) | 25.11 (+/–1.28) | 10.05 | |
| | 10h UV radiation | 34.54 (+/–1.08) | 9.10 (+/–0.37) | 20.98 (+/–1.10) | 2.91 | |
| Fe–Bentonite–HT | Before erosion | 40.95 (+/–0.06) | 19.36 (+/–0.19) | 20.49 (+/–0.73) | – | |
| | Hydrochloric acid | 32.57 (+/–0.33) | 18.97 (+/–0.69) | 15.10 (+/–1.14) | 9.97 | |
| | Sodium hydroxide | 27.93 (+/–0.03) | 17.25 (+/–0.06) | 21.86 (+/–0.04) | 13.26 | |
| | Alcohol | 35.56 (+/–0.43) | 20.90 (+/–0.02) | 19.61 (+/–0.04) | 5.67 | |
| | Toluene | 41.54 (+/–0.14) | 20.19 (+/–0.04) | 22.71 (+/–0.03) | 2.44 | |
| | 10h UV radiation | 40.52 (+/–0.29) | 18.90 (+/–0.24) | 22.11 (+/–0.15) | 1.73 | |
| Fe–Bentonite–PK | Before erosion | 29.82 (+/–0.69) | 24.66 (+/–1.70) | 21.06 (+/–2.89) | – | |
| | Hydrochloric acid | 27.36 (+/–0.01) | 23.94 (+/–0.10) | 21.70 (+/–0.14) | 2.64 | |
| | Sodium hydroxide | 29.79 (+/–0.75) | 17.68 (+/–0.68) | 13.68 (+/–1.28) | 10.16 | |
| | Alcohol | 30.01 (+/–0.04) | 26.81 (+/–0.04) | 24.16 (+/–0.03) | 3.77 | |
| | Toluene | 28.20 (+/–0.10) | 25.77 (+/–0.09) | 23.17 (+/–0.07) | 2.88 | |
| | 10h UV radiation | 29.17 (+/–1.03) | 25.97 (+/–0.86) | 23.38 (+/–0.60) | 2.74 | |

0.83 to 2.68, indicating that the color changes after erosion were either imperceptible or only slightly noticeable. In contrast, the pigment calcined at 500 °C showed significantly lower resistance, particularly to UV radiation ($\Delta E = 6.67$).

Table 2 presents data on bentonite-based pigments. The structure of bentonite underwent significant changes both during pigment synthesis via the hydrothermal method and after calcination, which is reflected in the color of the resulting pigments

Table 3. Colorimetric coordinates of Fe–Clinoptylolite hybrid pigments.

| Pigment | Solvents (solutions)/ UV radiation | $L*$ | a* | $b*$ | $\Delta E$ | Color |
|---|---|---|---|---|---|---|
| Clinoptilolite | – | 68.76 | -0.25 | 6.62 | – | |
| Fe–Clinoptilolite–P | Before erosion | 50.82 (+/–1.71) | 13.52 (+/–0.52) | 28.45 (+/–0.46) | – | |
| | Hydrochloric acid | 51.75 (+/–0.58) | 12.86 (+/–0.20) | 25.77 (+/–0.91) | 2.91 | |
| | Sodium hydroxide | 47.58 (+/–0.36) | 14.23 (+/–0.02) | 28.01 (+/–0.20) | 3.34 | |
| | Alcohol | 49.13 (+/–0.80) | 13.72 (+/–0.14) | 27.07 (+/–0.76) | 2.19 | |
| | Toluene | 49.87 (+/–0.07) | 13.45 (+/–0.10) | 27.19 (+/–0.62) | 1.58 | |
| | 10h UV radiation | 51.84 (+/–0.31) | 12.86 (+/–0.07) | 27.34 (+/–0.34) | 1.64 | |
| Fe–Clinoptilolite–HT | Before erosion | 50.98 (+/–3.67) | 14.39 (+/–3.44) | 14.06 (+/–8.20) | – | |
| | Hydrochloric acid | 47.21 (+/–0.11) | 20.73 (+/–0.05) | 23.46 (+/–0.15) | 3.77 | |
| | Sodium hydroxide | 45.71 (+/–0.05) | 19.09 (+/–0.15) | 26.65 (+/–0.10) | 5.27 | |
| | Alcohol | 46.20 (+/–0.16) | 21.18 (+/–0.03) | 25.51 (+/–0.11) | 4.78 | |
| | Toluene | 47.05 (+/–0.03) | 19.86 (+/–0.02) | 28.16 (+/–0.03) | 3.93 | |
| | 10h UV radiation | 45.63 (+/–0.15) | 19.32 (+/–0.16) | 26.14 (+/–0.28) | 5.35 | |
| Fe–Clinoptilolite–PK | Before erosion | 39.34 (+/–3.51) | 23.46 (+/–0.64) | 29.11 (+/–0.52) | – | |
| | Hydrochloric acid | 33.73 (+/–0.08) | 23.28 (+/–0.11) | 28.52 (+/–0.30) | 5.61 | |
| | Sodium hydroxide | 33.62 (+/–0.06) | 23.38 (+/–0.30) | 27.57 (+/–1.25) | 5.72 | |
| | Alcohol | 33.70 (+/–0.11) | 22.95 (+/–0.08) | 28.23 (+/–0.27) | 5.64 | |
| | Toluene | 33.69 (+/–0.29) | 23.27 (+/–0.07) | 28.82 (+/–0.16) | 5.65 | |
| | 10h UV radiation | 35.39 (+/–0.05) | 23.03 (+/–0.07) | 28.47 (+/–0.11) | 3.95 | |

and their stability (Table 2). The pigment calcined at 500 °C exhibits the highest $a^*$ value (24.66), similar to that observed for the kaolin-based pigment. The $a^*$ values of all synthesized pigments fall within the range reported in the literature for similar materials ($a^* = 9-36.8$) (Tian et al. 2017a; 2017b). Compared to kaolin-based pigments, bentonite-based pigments exhibit lower resistance to chemical reagents, particularly NaOH (Fe–Bentonite–PK – $\Delta E = 10.16$; Fe–Bentonite–HT – $\Delta E = 13.26$). The preparation method significantly influences the phase composition of the sample, and consequently, its color and stability. As a result of pigment synthesis via the hydrothermal method and calcination at 500 °C of the sample obtained by the precipitation method, the structure of bentonite was completely transformed – some reflections associated with montmorillonite disappeared, and new crystalline phases such as rokühnite and hematite emerged (Fig. 2).

Table 3 presents the colorimetric coordinates of pigments based on clinoptilolite. These pigments exhibited moderate resistance to chemical agents and UV radiation. Although the clinoptilolite structure remained largely intact during thermal treatments (hydrothermal synthesis and calcination at 500 °C), resistance to degradation decreased with increasing treatment temperature. The highest stability was observed for materials synthesized with the precipitation method and dried at 100 °C ($\Delta E = 1.58 - 3.34$), whereas the lowest stability was noted for materials calcined at 500 °C ($\Delta E = 3.95 - 5.72$).

## 4. CONCLUSIONS

The highest $a^*$ value, of approximately 24, was observed in pigments subjected to thermal treatment at 500 °C. This intense red coloration is attributed to the formation of hematite, as confirmed by XRD analysis. UV-Vis DR spectra further support this observation, revealing the presence of large $Fe_2O_3$ agglomerates (broad absorption band above 400 nm) in samples calcined at 500 °C – significantly more pronounced than in those dried at 100 °C or synthesized hydrothermally at 180 ° C. Although thermal treatment at 500 °C induced substantial structural transformations in the clay minerals, clinoptilolite retained its crystallographic structure after calcination. Kaolin–based pigments exhibited the highest resistance to chemical agents and UV radiation ($\Delta E = 0.83 - 6.67$), whereas bentonite-based pigments showed the lowest ($\Delta E = 1.73-13.26$). The greatest sensitivity to alkaline environments was observed in bentonite-based pigments synthesized via the hydrothermal method and those subjected to calcination at 500 °C. Overall, the color and stability of the pigments were strongly influenced not only by the type of clay mineral or zeolite used, but also by the synthesis method. Iron hybrid pigments prepared by using clay minerals (bentonite, kaolin) and clinoptilolite have unique properties that make them suitable for applications, especially in ceramic glazing, coatings, and paints. Iron-based pigments, composed of iron oxides such as hematite and goethite, are resistant to high temperatures, which makes them ideal for ceramic glazes fired at high temperatures. Iron-based pigments are widely used in ceramic glazes to achieve a range of colors – from earthy reds and browns to yellows and blacks – depending on firing conditions (oxidizing or reducing atmospheres) and iron concentration. Bentonite, due to its layered structure and ion-exchange capacity, serves as an ideal carrier for iron oxides. It also functions as a thickener, suspending agent, and thixotropic modifier, enhancing the consistency and stability of coatings, as well as improving application properties and adhesion to substrates. In paints, bentonite is employed as a rheology modifier, improving viscosity and preventing pigment settling. Iron pigments supported on a bentonite matrix impart natural hues and offer good UV resistance. Kaolin, on the other hand, enhances glaze smoothness and reduces cracking. In paints, kaolin is often used as a filler, enhancing opacity, texture, and viscosity, while also reducing formulation costs. Iron-modified kaolin is commonly used in decorative paints and coatings, providing soft, natural hues, matte finishes and improved UV resistance. Clinoptilolite is used in specialty glazes due to its ion-exchange properties, which help stabilize iron pigments and enhance glaze durability. Its zeolite structure can also contribute to subtle color variations. What is particularly important is that the obtained pigments are non-toxic and environmentally friendly, which aligns with current trends in the paint and coatings industry.

## SYMBOLS

| | |
|---|---|
| XRD | X-ray diffraction |
| UV-Vis DR | Ultraviolet–Visible Diffuse Reflectance Spectroscopy |
| CIE-L*a*b* | Commission Internationale de l'Éclairage L*a*b* color space |
| $L^*$ | lightness (0 is black and 100 is white) |
| $a^*$ | red–green axis (positive for red, negative for green) |
| $b^*$ | yellow–blue axis (positive for yellow, negative for blue) |

*Greek symbols*

| | |
|---|---|
| $\Delta E$ | the color difference between two samples in the CIE-L*a*b* color space |

## REFERENCES

Buyondo K.A, Kasedde H., Kirabira J.B., 2022. A comprehensive review on kaolin as pigment for paint and coating: recent trends of chemical-based paints, their environmental impacts and regulation. *Case Stud. Chem. Environ. Eng.*, 6, 100244. DOI: 10.1016/j.cscee.2022.100244.

Cunha R.V., Morais A.I.S., Trigueiro P., de Souza J.S.N., Damacena D.H.L., Brandão-Lima L.C., Bezerra R.D.S., Fonseca M.G., Silva-Filho E.C., Osajima J.A., 2023. Organic–inorganic hybrid pigments based on bentonite: strategies to stabilize the quinoidal base form of anthocyanin. *Int. J. Mol. Sci.*, 24, 2417. DOI: 10.3390/ijms24032417.

Dejoie C., Martinetto P., Dooryhée E., Strobel P., Blanc S., Bordat P., Brown R., Porcher F., del Rio M.S., Anne M., 2010. Indigo@silicalite: a new organic–inorganic hybrid pigment. *ACS Appl. Mater. Interfaces.*, 2, 2308–2316. DOI: 10.1021/am100349b.

Doula M.K., 2007. Synthesis of a clinoptilolite–Fe system with high Cu sorption capacity. *Chemosphere*, 67, 731–740. DOI: 10.1016/j.chemosphere.2006.10.072.

Fatah S.K., Aminian M.K., Bahamirian M., 2024. Enhancing colorant pigment properties of natural clinoptilolite zeolite through thermal treatment: comprehensive structural, optical, and colorimetric analysis. *J. Alloys Compd.*, 970, 172503. DOI: 10.1016/j.jallcom.2023.172503.

Grifasi N., Ziantoni B., Fino D., Piumetti M., 2024. Fundamental properties and sustainable applications of the natural zeolite clinoptilolite. *Environ. Sci. Pollut. Res.* DOI: 10.1007/s11356-024-33656-5.

Hosseini-Zori M., Taheri-Nassaj E., Mirhabibi A.R., 2008. Effective factors on synthesis of the hematite–silica red inclusion pigment. *Ceram. Int.,* 34, 491–496. DOI: 10.1016/j.ceramint.2006.11.012.

Khurana S., Kaur S., Kaur H., Khurana R.K., 2015. Multifaceted role of clay minerals in pharmaceuticals. *Future Sci. OA,* 1. DOI: 10.4155/fso.15.6.

Lu Y., Dong W., Wang W., Ding J., Wang Q., Hui A., Wang A., 2018. Optimal synthesis of environment-friendly iron red pigment from natural nanostructured clay minerals. *Nanomaterials*, 8, 925. DOI: 10.3390/nano8110925.

Mota-Heredia C., Cuevas J., Fernández R., 2024. Effect of iron chloride (II) on bentonites under hydrothermal gradients: a comparative study between sodium bentonite and calcium bentonite. *Minerals*, 14, 132. DOI: 10.3390/min14020132.

Niziurska N., Skokoń M., Ściślak S., Wieczorek W., Fendrych K., 2022. Analysis of influence of bentonite activation on its sorption properties. *Analit*, 12, 23–35.

Orolínová Z., Mockovčiaková A., 2009. Structural study of bentonite/iron oxide composites. *Mater. Chem. Phys.,* 114, 956–961. DOI: 10.1016/j.matchemphys.2008.11.014.

Pesando M., Bolzon V., Bulfoni M., Nencioni A., Nencioni E., 2022. Exploring the adsorption properties of zeolite in a new skin care formulation. *Cosmetics*, 9, 26. DOI: 10.3390/cosmetics9010026.

Pfaff G., 2022. 41 Iron oxide pigments, In: Pfaff G. (Ed.), *Volume 2 Color Measurement – Metal Effect Pigments*. De Gruyter, Berlin, Boston, 783–798. DOI: 10.1515/9783110587104-041.

Roy S., Kar S., Bagchi B., Das S., 2015. Development of transition metal oxide–kaolin composite pigments for potential application in paint systems. *Appl. Clay Sci.,* 107, 205–212. DOI: 10.1016/j.clay.2015.01.029.

Rutkowska M., Chmielarz L., Jabłońska M.,Van Oers C.J., Cool P., 2014. Iron exchanged ZSM-5 and Y zeolites calcined at different temperatures: activity in N2O decomposition. *J. Porous. Mater.,* 21, 91–98. DOI: 10.1007/s10934-013-9751-x.

Tian G., Wang W., Mu B., Wang Q., Wang A., 2017b. Cost-efficient, vivid and stable red hybrid pigments derived from naturally available sepiolite and halloysite. *Ceram. Int.*, 43, 1862–1869. DOI: 10.1016/j.ceramint.2016.10.145.

Tian G., Wang W., Wang D., Wang Q., Wang A., 2017a. Novel environment friendly inorganic red pigments based on attapulgite. *Powder Technol.,* 315, 60–67. DOI: 10.1016/j.powtec.2017.03.044.

Tora B., Kurzac M., Tajchman Z., 2009. Badanie możliwości uzyskania pigmentów żelazowych z odpadów metalurgicznych. *Rocznik Ochrona Środowiska*, 11, 571–582.

Wei S.-Y., Liu F., Feng X.-H., Tan W.-F., Koopal L.K., 2011. Formation and transformation of iron oxide–kaolinite associations in the presence of iron(II). *Soil Sci. Soc. Am. J.,* 75, 45–55. DOI: 10.2136/sssaj2010.0175.